

Geometric Phase Effects in the Vibrational Spectrum of $\text{Na}_3(X)$

Brian Kendrick

Theoretical Division (T-12, MS-B268), Los Alamos National Laboratory, Los Alamos, New Mexico 87545
(Received 14 April 1997)

The lowest 89 vibrational energy levels for $\text{Na}_3(X)$ for zero total angular momentum ($J = 0$) are computed both with and without the geometric phase. The calculations are full dimensional (3D) and utilize the vector potential (gauge theory) approach for including geometric phase effects. It is shown that the geometric phase leads to large shifts in the vibrational energy levels which result in a different ordering of states. These results can be verified experimentally and represent the first “clean” example of a geometric phase effect in molecular spectra. [S0031-9007(97)04174-4]

PACS numbers: 33.20.-t, 03.65.Bz

In 1963, Herzberg and Longuet-Higgins [1] showed that a Born-Oppenheimer electronic wave function changes sign for any closed path in the nuclear parameter space which encircles a conical intersection of two electronic potential energy surfaces (PESs). The geometrical interpretation of the sign change was first recognized by Mead and Truhlar [2] in 1979. They showed that the sign change can be expressed in terms of the “magnetic flux” due to a pseudomagnetic solenoid centered at the degeneracy point. Later, Mead [3] called this effect the “Molecular Aharonov-Bohm” effect. In 1984, Berry [4] showed that the sign change was a special case of a more general geometric phase factor, often referred to as “Berry’s Phase.” Because of the universal nature of this effect, Berry’s influential paper generated widespread interest [5] which continues to this day. Recent discussion of the geometric phase effect in molecules can be found in the review articles by Mead [6] and Yarkony [7].

For most molecules, calculations which accurately include the geometric phase are significantly more difficult than those which do not include it [8]. Because of these difficulties, there is currently widespread reluctance to include the geometric phase in scattering and bound state calculations. Instead, many hope that the effects of the geometric phase “wash out” when physical observables are calculated. Thus, explicit examples are needed which demonstrate the importance of the geometric phase and show when it must be included. It has recently been shown that (due to potential energy barriers and/or deep attractive wells) much simpler but approximate calculations which exclude the geometric phase can often provide extremely good agreement with experiment for *low* scattering or vibrational energies [8,9]. Thus, it is reasonable to compare exact calculations which include the geometric phase to approximate calculations which do not. In this way, we can quantify the “effects” of the geometric phase in real molecules.

As noted by Ham [10], probably the first experimentally verified example of a geometric phase effect was in crystal defects with strong Jahn-Teller coupling, where the lowest vibronic state was shown to have E symmetry instead of

A_1 or A_2 [11,12]. The first experimental verification of this ordering was for Cu^{2+} in MgO using electronic paramagnetic resonance [13]. This ordering is a direct consequence of the geometric phase. If it were not properly included, the opposite ordering would be predicted (i.e., the lowest vibronic state would be A_1 or A_2) [10]. Another interesting Jahn-Teller system for which the geometric phase alters the level ordering of the vibronic energy levels is the fullerene molecule C_{60} [14]. Significant geometric phase effects have also been found in $\text{H} + \text{H}_2$, $\text{H} + \text{D}_2$, and $\text{D} + \text{H}_2$ scattering at high energies [9]. General computational techniques which utilize the vector potential approach for including geometric phase effects were developed only recently [8]. These methods were applied to $\text{H} + \text{O}_2$ scattering and HO_2 bound state calculations and significant geometric phase effects were observed in the scattering results [8].

Geometric phase effects in molecular spectra (the topic of this paper) have also been investigated. The most popular candidates are the metal trimers Li_3 , Cu_3 , Na_3 , and K_3 for which relatively low-lying vibrational modes can readily encircle the D_{3h} conical intersection. Early treatments date back to Longuet-Higgins *et al.* [15] who correctly included the geometric phase in a model of a Jahn-Teller distorted molecule. The first calculations to treat a real molecule (Li_3) were performed by Gerber and Schumacher [16]. The vibrational spectra of Cu_3 both in an excited electronic state and in its ground state have also been computed [17]. All of these previous calculations included the geometric phase by diagonalizing an approximate two-state diabatic Hamiltonian. As expected, the lowest vibronic state for these systems was found to be of E symmetry. However, the conical intersection in Li_3 and Cu_3 lies very low in energy, which gives rise to large nonadiabatic coupling. This coupling leads to additional energy shifts which mix with those due to the geometric phase. Thus, these two systems do not provide a “clean” example of the geometric phase effect in molecular spectra. Notably lacking is a clean example which quantifies the effects of the geometric phase in the vibrational spectrum of a real molecule. Fortunately,

clean examples are provided by the Na_3 and K_3 metal trimers whose ground electronic states exhibit conical intersections which lie much higher in energy. Thus, the adiabatic approximation is valid for these two molecules, and a calculation of the low-lying vibrational states using a single ground state electronic PES is possible.

The Na_3 metal trimer has been under intense theoretical [18–22] and experimental [23–26] investigation in recent years, but almost all interest has been focused on the nuclear dynamics in the excited B electronic state. In fact, the vibrational spectrum of $\text{Na}_3(B)$ was originally believed to be the first example of the geometric phase effect in molecular spectra [24]. However, in recent years more detailed theoretical treatment [20] and higher resolution spectroscopy [26] have reversed this original claim. It is now clear that there is *no* geometric phase effect in the vibrational spectra for the B electronic state. The B state is of ${}^2A'_1$ symmetry (instead of ${}^2E'$ as was once thought) and exhibits an *avoided* crossing at the D_{3h} geometry with a nearby ${}^2E'$ doubly degenerate state. Thus, the vibrational wave functions are single valued, and the spectra can be classified using a pseudo-Jahn-Teller coupling scheme [20]. Interestingly, the nuclear dynamics on the ground electronic state [$\text{Na}_3(X)$] has received very little attention even though it is well known that a conical intersection is located at the equilateral triangular configuration (D_{3h} symmetry) [18,19]. This paper presents the results of the first full dimensional (3D) calculation of the vibrational spectrum of $\text{Na}_3(X)$ both with and without the geometric phase using a realistic PES. As shown below, the low-lying vibrational energies of $\text{Na}_3(X)$ are well approximated by simpler calculations which exclude the geometric phase. However, an accurate treatment which includes the geometric phase is necessary in order to obtain agreement between theory and experiment for the intermediate and high-lying vibrational states.

The vibrational energies for $\text{Na}_3(X)$ including geometric phase effects were computed by solving the generalized Born-Oppenheimer equation for the *complex* single-valued nuclear wave functions $\Psi^C(x)$ [2,8,22]

$$\left\{ \frac{\hbar^2}{2\mu} [-i\nabla_x - \mathbf{A}(x)]^2 + V(x) \right\} \Psi^C(x) = E\Psi^C(x), \quad (1)$$

where $V(x)$ is the ground state electronic PES for $\text{Na}_3(X)$ [18,19] and $\mathbf{A}(x)$ is the relevant vector potential for a D_{3h} conical intersection [2,8,22]. In practice, hyperspherical coordinates $x = (\rho, \theta, \phi)$ are used, and the explicit form of Eq. (1) in these coordinates is given in Ref. [8]. A contour plot of the PES for $\text{Na}_3(X)$ for a fixed value of the hyperradius $\rho = 8.71a_0$ is shown in Fig. 1. Motion along the hyperradius ρ corresponds to the symmetric stretch mode (ν_1). In the bottom of the well just left of the origin, motion along the x axis corresponds to the bending mode (ν_2) and motion along the y axis corresponds to the antisymmetric stretch mode (ν_3). Motion along the azimuthal coordinate ϕ about the origin corresponds to a pseudoro-

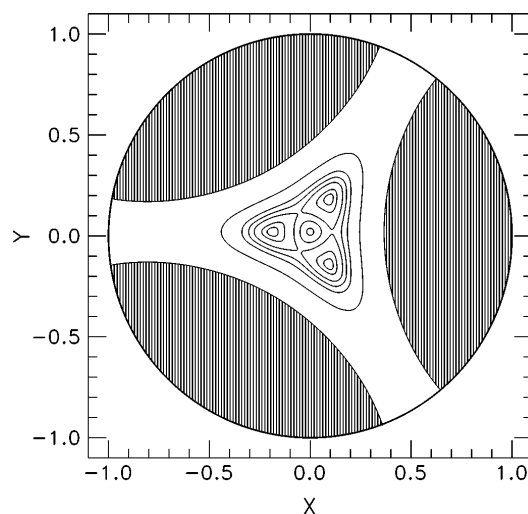


FIG. 1. Contour plot of the $\text{Na}_3(X)$ PES with the hyperradius ρ fixed at $8.71a_0$. This is a stereographic projection of the surface of an upper half-sphere. The hyperangle θ runs from 0 at the north pole (center of plot) to $\frac{\pi}{2}$ at the equator (heavy circle). The hyperangle ϕ , the azimuthal angle, is measured from the positive x axis and grows going counterclockwise. Repulsive regions where the potential energy is greater than $20,000 \text{ cm}^{-1}$ are shaded. The contours are at 25, 100, 300, 500, 800, and 2000 cm^{-1} , and all energies are measured relative to the bottom of the wells.

tational motion. The D_{3h} conical intersection is located at the origin of the plot which corresponds to an equilateral triangular configuration. The threefold symmetry gives rise to three wells which are equally spaced at 120° intervals around the origin. The minimum energies relative to the bottom of the wells for the pseudorotational barrier (i.e., the saddle points between the three wells) and the conical intersection are 292.6 and 962.1 cm^{-1} , respectively.

Equation (1) was solved using a newly developed DVR/FBR (Discrete Variable Representation/Finite Basis Representation) numerical technique which is described in detail elsewhere [8,22]. The appropriate projection operator was then applied to the *complex* solutions to obtain *real* (double-valued) solutions with the desired permutation symmetry [8,22]. The state assignments (ν_1, ν_2, ν_3) were determined by a visual inspection of the nodal patterns of several 2D slices of the 3D wave function for each vibrational state. The A_1 , A_2 , and E vibrational energies and state assignments computed both with and without the geometric phase are presented in Figs. 2, 3, and 4, respectively. The approximate results which exclude the geometric phase (NGP) correspond to setting $\mathbf{A} = 0$ in Eq. (1) [8]. The vibrational wave functions for the exact GP results are double valued so that the A_1 (A_2) states are simultaneously symmetric (antisymmetric) across the wells and antisymmetric (symmetric) across the saddle points [22]. The vibrational wave functions for the approximate NGP results are single valued so that the A_1 (A_2) states

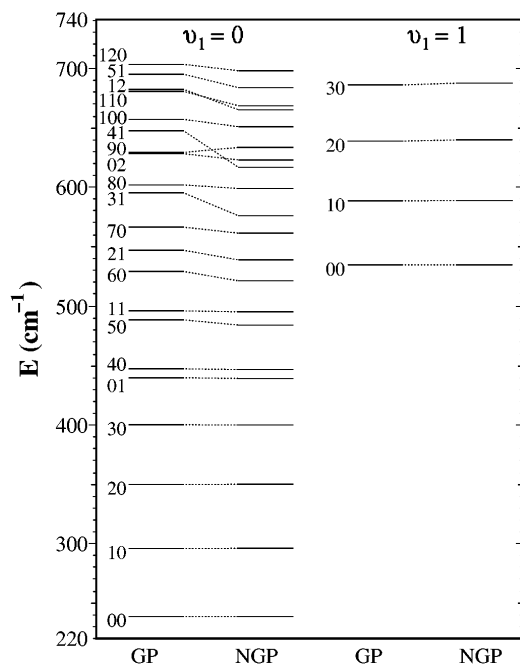


FIG. 2. Plot of the lowest 25 nondegenerate vibrational energies of A_1 symmetry for zero total angular momentum ($J = 0$). The symmetry designation denotes the symmetry behavior of the double-valued wave functions across the wells. The exact results, which include the geometric phase, are denoted by geometric phase (GP), and the approximate results which exclude it are denoted by no geometric phase (NGP). The energy levels are grouped into two columns labeled by the symmetric stretch quantum number ν_1 . The bending (ν_2) and asymmetric stretch (ν_3) quantum numbers are given by the pair of numbers ($\nu_2\nu_3$) beside each GP energy level. The dotted lines connect the GP energies to the corresponding NGP energies. All energies are relative to the bottom of the wells.

are symmetric (antisymmetric) across both the wells and saddle points. Detailed convergence studies indicate that the relative error for the lowest ten energy levels is $<0.3 \text{ cm}^{-1}$ while for the higher levels it is $<1.0 \text{ cm}^{-1}$ (i.e., less than the width of the lines in Figs. 2–4). Thus, any visible differences between the energy levels for the exact GP and approximate NGP results are real and due entirely to the geometric phase. The ground state energies for the A_1 and E states are identical (238.5 cm^{-1}) and are the only states which lie below the pseudorotational barrier. The other low-lying states of A_1 , A_2 , and E symmetry lie above the pseudorotational barrier, but their wave functions remain localized over the attractive wells, and the approximate NGP results are still in excellent agreement with the exact GP results. However, for the intermediate to high-lying states, the wave functions become delocalized and we see significant energy shifts between the exact GP and approximate NGP results. Most notable is the change in the ordering of the 041 and 012 states of A_1 symmetry, the 040, 050, and 012 states of A_2 symmetry, and the 061 and 101 states of E symmetry.

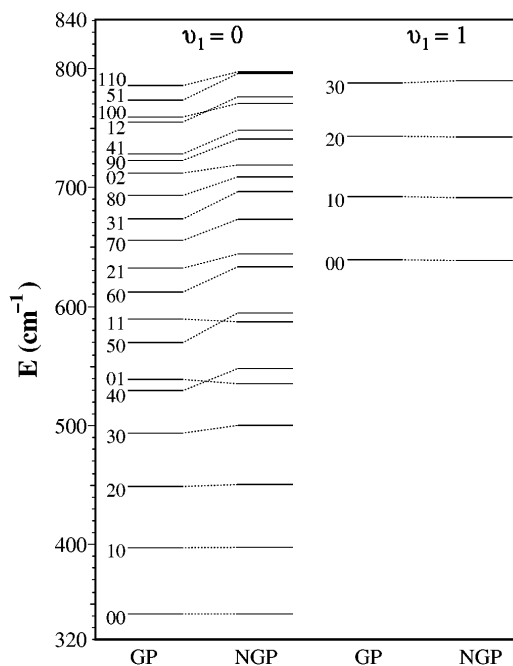


FIG. 3. Same plot as in Fig. 2, except that the lowest 24 nondegenerate vibrational energies of A_2 symmetry are plotted.

The only experimental results to date for the vibrational energy levels of $\text{Na}_3(X)$ are based on two-photon ionization spectra of the hot bands [25]. The three lowest vibronic energies (relative to the ground state) are reported to be $\omega_1 = 139.0 \text{ cm}^{-1}$, $\omega_2 = 49.5 \text{ cm}^{-1}$, and

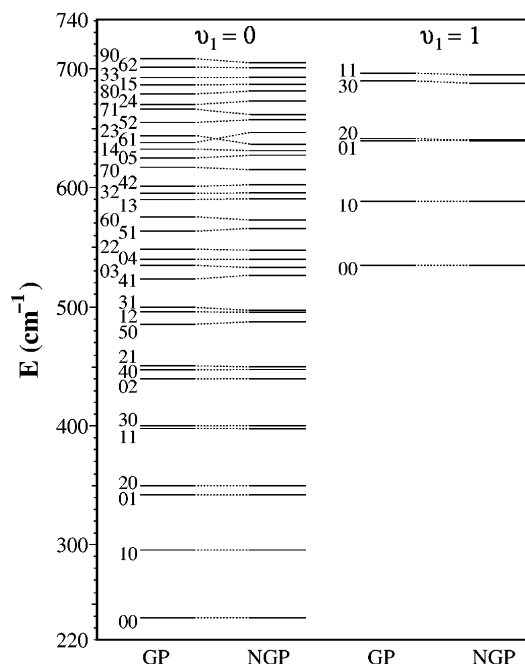


FIG. 4. Same plot as in Fig. 2, except that the lowest 40 doubly degenerate vibrational energies of E symmetry are plotted.

$\omega_3 = 87.0 \text{ cm}^{-1}$. The only theoretical results to date are based on a crude harmonic oscillator approximation [19]. They find $\omega_1 = 142.0 \text{ cm}^{-1}$, $\omega_2 = 58.0 \text{ cm}^{-1}$, and $\omega_3 = 94.0 \text{ cm}^{-1}$, which are in surprisingly good agreement with the experimental results. Both of the previous experimental and theoretical treatments *assume* that the three lowest energies are the fundamentals. The present *E* symmetry results in Fig. 4 give $\omega_1 = 295.3 \text{ cm}^{-1}$, $\omega_2 = 56.9 \text{ cm}^{-1}$, and $\omega_3 = 102.9 \text{ cm}^{-1}$, which agree with the previous assignments for the fundamental bend (010) and asymmetric stretch (001) modes but disagree with the previous assignment for the symmetric stretch (100) mode. The *E* symmetry energy level in Fig. 4, which is closest to the observed 139.0 cm^{-1} energy level, is the 011 state with a calculated relative energy of 158.7 cm^{-1} . By replacing the theoretical energy spacings for the 010 and 001 states in Fig. 4 with the experimental ones, the experimental energy for the 011 state can be estimated as $49.5 + 87.0 = 136.5 \text{ cm}^{-1}$, which is indeed very close to 139 cm^{-1} . Therefore, the present calculations suggest that the observed 139.0 cm^{-1} energy level should be reassigned as the 011 state. The discrepancies between the current theoretical energies and experiment are due to errors in the PES for $\text{Na}_3(X)$. Future calculations on an improved surface will give more quantitative agreement. However, since improvements in the PES will affect both the GP and NGP results the same, the large relative energy shifts and state reordering observed between the GP and NGP results in Figs. 2–4 will remain. Thus, the state ordering predicted by the present GP results for the vibrational energies of $\text{Na}_3(X)$ could be verified experimentally [27]. The present results clearly show that $\text{Na}_3(X)$ is a good candidate for studying geometric phase effects and that its vibrational spectrum provides the first clean example of this effect in molecular spectra.

I thank R. T. Pack for his helpful comments and suggestions, and the members of group T12 at Los Alamos for allowing these computations to be distributed over many of their workstations.

-
- [1] G. Herzberg and H. C. Longuet-Higgins, *Discuss. Faraday Soc.* **35**, 77 (1963).
 [2] C. A. Mead and D. G. Truhlar, *J. Chem. Phys.* **70**, 2284 (1979); C. A. Mead, *J. Chem. Phys.* **72**, 3839 (1980).
 [3] C. A. Mead, *Chem. Phys.* **49**, 23 (1980).

- [4] M. V. Berry, *Proc. R. Soc. London A* **392**, 45 (1984).
 [5] *Geometric Phases in Physics*, edited by A. Shapere and F. Wilczek (World Scientific, Singapore, 1989).
 [6] C. A. Mead, *Rev. Mod. Phys.* **64**, 51 (1992).
 [7] D. R. Yarkony, *Rev. Mod. Phys.* **68**, 985 (1996).
 [8] B. Kendrick and R. T. Pack, *J. Chem. Phys.* **104**, 7475 (1996); **104**, 7502 (1996); **106**, 3519 (1997).
 [9] Y. M. Wu and A. Kuppermann, *Chem. Phys. Lett.* **201**, 178 (1993); **235**, 105 (1995); A. Kuppermann, in *Dynamics of Molecules and Chemical Reactions*, edited by R. E. Wyatt and J. Z. H. Zhang (Marcel Dekker, New York, 1996), and references therein.
 [10] F. S. Ham, *Phys. Rev. Lett.* **58**, 725 (1987).
 [11] M. C. M. O'Brien, *Proc. R. Soc. London A* **281**, 323 (1964).
 [12] The symmetry designations *E*, *A*₁, and *A*₂ refer to the three irreducible representations of the group *S*₃ (the permutation group for three identical particles).
 [13] R. E. Coffman, *Phys. Lett.* **19**, 475 (1965); **21**, 381 (1966); *J. Chem. Phys.* **48**, 609 (1968).
 [14] A. Auerbach, N. Manini, and E. Tosatti, *Phys. Rev. B* **49**, 12998 (1994); **49**, 13008 (1994); A. Auerbach, *Phys. Rev. Lett.* **72**, 2931 (1994).
 [15] H. C. Longuet-Higgins, U. Öpik, M. H. L. Pryce, and R. A. Sack, *Proc. R. Soc. London A* **244**, 1 (1958).
 [16] W. H. Gerber and E. Schumacher, *J. Chem. Phys.* **69**, 1692 (1978).
 [17] T. C. Thompson, D. G. Truhlar, and C. A. Mead, *J. Chem. Phys.* **82**, 2392 (1985); *Chem. Phys. Lett.* **127**, 287 (1986).
 [18] R. L. Martin and E. R. Davidson, *Mol. Phys.* **35**, 1713 (1978); J. L. Martins, R. Car, and J. Buttet, *J. Chem. Phys.* **78**, 5646 (1983).
 [19] T. C. Thompson, G. Izmirlan, Jr., S. J. Lemon, D. G. Truhlar, and C. A. Mead, *J. Chem. Phys.* **82**, 5597 (1985).
 [20] R. Meiswinkel and H. Köppel, *Chem. Phys.* **144**, 117 (1990); J. Schön and H. Köppel, *Chem. Phys. Lett.* **231**, 55 (1994); *J. Chem. Phys.* **103**, 9292 (1995).
 [21] B. Reischl, *Chem. Phys. Lett.* **239**, 173 (1995).
 [22] B. Kendrick, *Int. J. Quantum Chem.* (to be published).
 [23] A. Herrmann, M. Hofmann, S. Leutwyler, E. Schumacher, and L. Wöste, *Chem. Phys. Lett.* **62**, 216 (1979).
 [24] G. Delacrétaz, E. R. Grant, R. L. Whetten, L. Wöste, and J. W. Zwanziger, *Phys. Rev. Lett.* **56**, 2598 (1986).
 [25] M. Broyer, G. Delacrétaz, P. Labastie, J. P. Wolf, and L. Wöste, *J. Phys. Chem.* **91**, 2626 (1987).
 [26] W. E. Ernst and S. Rakowsky, *Ber. Bunsen-Ges. Phys. Chem.* **99**, 441 (1995).
 [27] Experiments based on resonant two-photon ionization (R2PI) spectroscopy, dispersed fluorescence spectroscopy, and Raman spectroscopy could be used to verify the present results. Future calculations for nonzero total angular momentum ($J \neq 0$) will give results which could be verified using infrared spectroscopy.